[CANCER RESEARCH 61, 6540–6547, September 1, 2001]

Overexpression of IRF9 Confers Resistance to Antimicrotubule Agents in Breast Cancer Cells[1]

Kathryn E. Luker, Christina M. Pica, Robert D. Schreiber, and David Piwnica-Worms[2,3]

Departments of Radiology [K. E. L., C. M. P., D. P-W.], Molecular Biology and Pharmacology [K. E. L., C. M. P., D. P-W.], and Pathology and Immunology [R. D. S.], Washington University Medical School, St. Louis, Missouri 63110

ABSTRACT

IRF9/p48/ISGF3γ (IRF9) is an IFN regulatory factor that mediates signaling by type I IFNs (IFNα and IFNβ). After single-step selection of breast adenocarcinoma cells in paclitaxel, differential display and single gene analysis demonstrated that transcriptional activation of IRF9 and other IFN-responsive genes, independent of IFN, corresponded with resistance to antimicrotubule agents. Transient overexpression of IRF9 reproduced the drug-resistance phenotype and induced expression of IFN-responsive genes. However, drug resistance was not induced by overexpression of Stat1 or Stat2, or treatment with IFNα *per se*. Using a donor-matched array of cDNA prepared from human tumor and normal tissue from a variety of organs, we observed overexpression of IRF9 in approximately one-half of breast and uterine tumors, which indicated that IRF9 may be important in signaling in these tumor types. These data identify a novel IFN-independent role for IRF9 in the development of resistance to antimicrotubule agents in breast tumor cells and may link downstream mediators of IFN signaling to drug resistance in human cancers.

INTRODUCTION

Antimicrotubule agents interfere with the formation of the mitotic spindle, causing cell cycle arrest at the spindle assembly checkpoint (1). Microtubule destabilizing agents (nocodazole and *Vinca* alkaloids such as vinblastine) prevent attachment of kinetochores to spindle poles (2), whereas taxanes (paclitaxel, docetaxel) and epithilones stabilize microtubules, preventing depolymerization of tubulin subunits and causing a loss of tension at kinetochores but no apparent disturbance of microtubule-kinetochore attachment (3). In the absence of a normal mitotic spindle, cells with an intact spindle assembly checkpoint do not progress to anaphase. Instead, arrested cells may die (through apoptosis or mitotic cell death) or alternatively may survive either to exhibit a SLP[4] (4) or to resume proliferation in a potentially aneuploid state (5). Although the factors controlling the outcome of abnormal mitosis remain unclear, a complex regulatory system is emerging involving a number of proteins important in cell cycle control and apoptosis, the most central of which are p53, p21/cip1, bcl-2, and pro-apoptotic bcl-2 family members such as bax and bcl-x (6).

Among antitumor agents directed against microtubules, paclitaxel is the most widely used, with clinical efficacy against a number of malignancies, including breast, ovarian, and lung carcinoma. Paclitaxel has been used extensively in studies to identify proteins and processes involved in cell survival after prolonged mitotic arrest (7, 8). Resistance to paclitaxel has been reported to be conferred by overexpression of bcl-2 (9) or p21/cip1 (10). Conversely, paclitaxel cytotoxicity appears to be enhanced by p53 mutation (11) and expression of bcl-x_s (12). Induction of terminal proliferation arrest (SLP), rather than apoptosis, also has been shown to be positively regulated by p21 and p53 (13). Overall, these studies have focused on mechanisms conferring cell survival as a measure of drug resistance. However, less is known about the proliferative capacity (clonogenicity) of surviving cells, a feature of drug resistance that may have greater clinical significance (14).

In the present study, we investigated mechanisms of drug resistance in sublines of MCF-7 breast tumor cells derived by single-step selection with paclitaxel and clonogenic expansion. Using differential display, a paclitaxel-resistant cell line was shown to constitutively overexpress several proteins regulated by type I IFN in the absence of IFN. At the center of this pathway was the IFN regulatory factor IRF9/p48/ISGF3γ (IRF9), which we show can function independently of IFN as a positive regulator of resistance to antimicrotubule agents.

MATERIALS AND METHODS

Cells. MCF-7 breast adenocarcinoma cells and derivatives were cultured in DMEM (Life Technologies, Inc., Grand Island, NY) with 10% FCS, 2 mM L-glutamine, and 0.1% penicillin/streptomycin. WISH cells were grown in DMEM with 10% heat-inactivated FCS, 2 mM L-glutamine, 1% nonessential amino acids, 1% pyruvate, and 0.1% penicillin/streptomycin. NIH 3T3 mouse fibroblasts, stably transfected with human *MRP1* (gift of Gary Kruh, Fox Chase Cancer Center, Philadelphia, PA), were maintained in DMEM (Life Technologies, Inc.) with 10% heat-inactivated FCS, 2 mM L-glutamine, and 0.1% penicillin/streptomycin and were passaged once per month in 750 μg/ml G418. KB-8–5-11 multidrug-resistant epithelial carcinoma cells (15) were cultured in the same medium with 100 ng/ml colchicine. The MRP1 transfectants and KB-8-5-11 cells served as positive controls in Western blots for MRP1 and MDR1, respectively.

Reagents. Paclitaxel, vinblastine, and doxorubicin were obtained from Sigma Chemical Co. (St. Louis, MO), and stocks were prepared in DMSO. A stock solution of GF120918 (gift of Glaxo-Wellcome, Research Triangle Park, NC) was prepared in DMSO. IFNα, derived from human leukocytes, was obtained from Sigma Chemical Co. Plasmid pCMV-Ad-IRF9 was a gift from D. E. Levy, New York University, New York, NY, and plasmids RcCMV-Stat1 p91 and pcDNA3-Stat2 were gifts from J. Darnell, Rockefeller University, New York, NY.

Fluctuation Analysis. A fluctuation analysis-style selection of MCF-7 variants was performed essentially as described previously (16). Cells were expanded from 2000 to an average of 1.9×10^6 in 15 independent populations. Each population was exposed to 72 nM paclitaxel for 7 days. After 3 weeks of recovery in medium without paclitaxel, colonies were counted.[1] The variation rate (or mutation rate), *a*, was calculated by the method of means, according the following equation:

$$r = aN \ln(NCa)$$

where *r* is the mean number of variant cells per parallel culture present at the time of selection (the mean number of resistant colonies), *C* is the number of parallel cultures, and *N* is the average number of cells per culture at the time of selection (17, 18).

Received 1/23/01; accepted 7/3/01.

The costs of publication of this article were defrayed in part by the payment of page charges. This article must therefore be hereby marked *advertisement* in accordance with 18 U.S.C. Section 1734 solely to indicate this fact.

[1] Supplementary data for this article is available at *Cancer Research Online* (http://cancerres.aacrjournals.org).

[2] Supported by grants from the United States Department of Energy (DE-FG02-94ER61885) and NIH (P20 CA86251). K. E. L. was recipient of a 2001 AFLAC Travel Award to present an abstract of this work at the 92nd Annual Meeting of the AACR.

[3] To whom requests for reprints should be addressed, at Molecular Imaging Center, Mallinckrodt Institute of Radiology, Washington University Medical School, 510 South Kingshighway Boulevard, Box 8225, St. Louis, MO 63110. Phone: (314) 362-9356; Fax: (314) 362-0152; E-mail: piwnica-wormsd@mir.wustl.edu.

[4] The abbreviations used are: SLP, senescence-like phenotype; BrdUrd, bromodeoxyuridine; Pgp, P-glycoprotein; PI, propidium iodide; MDR1, multidrug resistance gene-1; MRP1, multidrug resistance-associated protein-1; CPE, cytopathic effect.

Cytotoxicity Assays. MCF-7 cells and variants from nonconfluent flasks were trypsinized and passed through a 22-gauge needle prior to counting. Cells (5000/well) were plated in 96-well microtiter plates and permitted to adhere. After 24 h, drugs were added to the medium at the indicated final concentration (drug vehicle, 0.1% DMSO). Cell protein was quantified 72 h after drug addition with sulforhodamine B. IC_{50} values were calculated by computer fit of the data using SigmaPlot (19).

Clonogenic Assays. MCF-7 cells and variants were seeded on day 0. After 24 h, drug was added to the medium at the indicated final concentrations (day 1). Medium containing drug was replaced on days 3 and 5. On day 8, cells were washed with PBS and fed with fresh medium without drug. Medium was replaced every 72–96 h for the remainder of the experiment. Cells were monitored daily by light microscopy for small colonies of proliferating cells. No evidence of proliferation was observed in MCF-7 cells or any of the sublines tested until ~10–14 days after removal of paclitaxel. Colonies were counted 3–4 weeks after the removal of drug by staining with Coomassie Brilliant Blue. Cell clusters ≥50 cells were defined as colonies.

For clonogenic assays in the presence of IFNα, MCF-7 (7.5×10^6/T162) and 11C9 cells (1×10^6/T75) were seeded in the presence of 0, 1, 10, or 100 units/ml human IFNα and maintained in IFNα throughout paclitaxel selection and recovery. Paclitaxel (100 nM) was added to the culture medium 24 h after plating. Selection and colony counts were performed as above.

Clonogenic assays using transiently transfected cells were performed as above with the following exceptions. Cells (6×10^5/10-cm dish or 2×10^5/6-cm dish) were seeded and transfected after 24 h with 6 μg of pCMV-Ad-IRF9, RcCMV-Stat1 p91, pcDNA3-Stat2, or pcDNA6-V5-His-LacZ using FuGene-6 (Roche Molecular Biochemicals, Indianapolis, IN) according to manufacturer's instructions. Transfection efficiency was 25–30% under these conditions as measured by transfection of cells with pcDNA6-V5-His-lacZ (Invitrogen, Carlsbad, CA) and staining with X-gal (5-bromo-4-chloro-3-indolyl β-D-galactopyranoside). Paclitaxel (100 nM) or vinblastine (1 μM) were added 48 h after transfection.

Western Blots. Western blots were prepared with whole cell lysates of subconfluent cultures of cells, with the exception of Western blots for Pgp and MRP1, which were performed using enriched membrane preparations as described previously (20, 21). Mouse monoclonal antibodies against IRF9, Bcl-2, Bcl-x, MCH-3/caspase-7, CPP32/caspase-3, Kip-1/p27, and Cip-1/Waf-1/p21 were obtained from BD Transduction Laboratories, San Diego, CA. Rabbit polyclonal antibodies against IRF-1 and Stat2 (C-20) and mouse monoclonal antibodies against Stat1 p84/p91 (C-136) and p53 were obtained from Santa Cruz Biotechnology, Inc., Santa Cruz, CA. Mouse monoclonal antibodies against Pgp (C219) and MRP1 (QCLR-1) were obtained from Signet Laboratories, Dedham, MA. Binding of primary antibodies against IRF9, Stat1, Stat2, and IRF1 was visualized using antirabbit or antimouse IgG conjugated to alkaline phosphatase (Santa Cruz Biotechnology) with nitro blue tetrazolium (NBT) and 5-bromo-4-chloro-3-indolyl phosphate (BCIP). Binding of all other antibodies was visualized using antimouse IgG conjugated to horseradish peroxidase (Amersham Pharmacia Biotech, Piscataway, NJ) and enhanced chemiluminescence (Amersham Pharmacia Biotech).

Cellular Accumulation of Radiotracers. Transport activity and modulation of *MDR1* Pgp were assayed with ^{99m}Tc-Sestamibi as described previously (22). ^{99m}Tc-Sestamibi was prepared with a one-step kit formulation (Cardiolite; DuPont Medical Products Division, Wilmington, DE) as described previously (22). Cells were seeded on 20-mm coverslips at a density of 1×10^6 per 10-cm dish and were allowed to adhere for 24 h. Experiments were performed by equilibrating coverslips with cells for 30 min in modified Earles' balanced salt solution transport buffer containing ^{99m}Tc-Sestamibi (10 pM; 7.5 pmol/mCi) in the presence or absence of GF120918 (300 nM). This concentration of GF120918 is sufficient to maximally inhibit *MDR1* Pgp in a number of cell lines (23). Preparations were then washed, extracted, and analyzed for protein content and γ activity (22). Data are reported as fmol Tc-Sestamibi (mg protein)$^{-1}$ (nM$_o$)$^{-1}$, where nM$_o$ represents total concentration of Tc-Sestamibi in the extracellular buffer.

Assays of [^{3}H]paclitaxel accumulation were performed as above with the following exceptions. Coverslips were incubated in transport buffer containing 100 nM [^{3}H]paclitaxel (Moravek Biochemicals, Brea, CA; 10 Ci/mmol) in 0.1% ethanol (final) or vehicle alone for various times. For quantitation of [^{3}H]paclitaxel, cell lysates were added to scintillation mixture (Redi-Solv; Beckman Coulter, Inc., Fullerton, CA).

Flow Cytometry. For 96-h time course studies of cell cycle arrest mediated by paclitaxel, 600,000 cells per 10-cm dish were plated and allowed to adhere for 24 h before the addition of 100 nM paclitaxel. At the indicated times, medium was removed and retained, adherent cells were trypsinized, and the suspended and adherent cells were combined and washed with PBS and then fixed with 70% ethanol prior to staining with PI. For each time point, 10,000 events were recorded using a FacsCalibur flow cytometer (Becton Dickinson Immunocytometry Systems, San Diego, CA).

Long-term response to paclitaxel was measured using subconfluent monolayers in T162 flasks treated with 100 nM paclitaxel. Medium containing drug was added on day 1 and replaced on days 3 and 5. On day 8, the cells were washed with PBS and fed fresh medium without drug. Medium was replaced every 3rd day for the remainder of the experiment. For detection of cells in S phase, BrdUrd (Amersham Pharmacia Biotech) was added to the medium at a final concentration of 10 nM 4 h prior to trypsinization (and 24 h after feeding). Cells were trypsinized at the indicated times, washed with PBS, and fixed with ethanol. Fixed cells were washed and stained with anti-BrdUrd antibody conjugated to FITC (Roche) and PI. For each point, 50,000 events were recorded.

Flow cytometric analysis of MHC class I cell surface expression was performed according to the manufacturer's recommendations using FITC-conjugated anti-HLA-A,B,C (G46–2.6) mouse monoclonal antibody recognizing MHC class I (BD PharMingen, San Diego, CA). Cells were seeded and remained untreated or were either treated with 1000 units of IFNα/ml for 72 h or transfected with various plasmids 24 h after seeding. In all cases, cells were stained 96 h after seeding. Cells were trypsinized, washed in PBS (pH 7.5) with 1% serum, and incubated for 20 min on ice in PBS containing 1% serum and anti-HLA-A,B,C antibody. Cells were then washed in PBS with 1% serum and analyzed by flow cytometry using a FacsCalibur flow cytometer. Duplicate labeling reactions were prepared for each dish of cells in addition to an unstained control. Fold increase in class I expression was calculated as the ratio of mean fluorescence intensity of treated cells:untreated parental cells in the same experiment.

IFN CPE Assays. Assays of protection from viral infection were performed essentially as described previously (24). WISH cells (7500/well) were seeded in 96-well plates. On the day of seeding, human IFNα (0.1–1000 units/ml) or medium taken from 72 h cultures of MCF-7 or 11C9 cells (maximum concentration, 0.5×) was added to the wells. After 24 h of incubation, cells were washed in warm PBS (pH 7.5), and fresh prewarmed medium containing vesicular stomatitis virus (VSV) was added. After 48–72 h, medium was removed, and live cells were quantitated by crystal violet staining.

Differential Display. Total RNA was isolated from MCF-7 cells and 11C9 cells (untreated and after 7 days of 100 nM paclitaxel + 15-day recovery in drug-free medium) by modified phenol/chloroform extraction with Trizol (Life Technologies, Inc.). DNA was removed by DNase digestion (MessageClean kit; GenHunter, Nashville, KY). Reverse transcription was performed, and the resulting cDNA was used for subsequent random primed PCR (RNAimage kits 1–10; GenHunter). PCR was performed using 240 primer combinations using [α-^{33}P]dATP. Samples were electrophoresed on polyacrylamide gels (6%), which were dried and subjected to autoradiography. Reactions producing differences in banding patterns between MCF-7 and 11C9 samples were repeated, and 21 bands representing reproduced differences were excised from the dried gels. DNA was extracted with water from the excised bands and amplified using primers specific to the originating reaction. The resulting amplified products were electrophoresed on agarose gels and bands corresponding to the predicted molecular weight were excised from the gels and ligated into a PCR cloning plasmid, pNoTAT7 (PrimePCR cloning kit; Eppendorf Scientific, Westbury, NY). The sequences of cDNA inserts in plasmids from three colonies per ligation were compared with the GenBank nonredundant and EST databases using the BLAST algorithm (25).

Differences were first screened by reverse Northern dot blot. Radiolabeled total cDNA was produced by reverse transcription with [α-^{32}P]dCTP from the original total RNA preparations for untreated MCF-7 and 11C9 cells (ReversePrime kit; GenHunter). Duplicate dot blots were prepared from the clones of interest and hybridized with each labeled cDNA according to the manufacturer's recommendations.

Northern blots were prepared by electrophoresing 5 μg of total RNA in formaldehyde gels and blotting by capillary transfer. Probe DNA was cut

from the plasmid clones using suitable restriction enzymes in the polylinker of the PCR cloning plasmid, and inserts were gel purified and labeled with [α-^{32}P]dATP using the random hexamer method (HotPrime kit; GenHunter). Radiolabeled probes were hybridized with blots according to the manufacturer's directions. GenBank accession numbers for human cDNAs are: MxA (M30817), hepatitis C-associated microtubular aggregate protein p44 (SEG_HUMHCAMAP), IFI27 (NM_005532), and KIAA0069 (D31885).

Matched Tumor/Normal Expression Array. A matched tumor/normal tissue expression array (Clontech Laboratories, Inc., Palo Alto, CA) containing cDNA prepared from 68 untreated human tumors with matched normal tissue from each individual was hybridized according to the manufacturer's directions with a full-length IRF9 probe labeled with [α-^{32}P]dATP as above. Hybridization signals were quantified using a PhosphorImager (Amersham Molecular Dynamics) with each spot interrogated by volume analysis and background subtraction. The blot was stripped of bound radioactivity according to manufacturer's directions and hybridized with a ubiquitin probe (Clontech) labeled with [α-^{32}P]dATP as above. Bound radioactivity was again quantified using the PhosphorImager. Autoradiographs were exposed for 72 h for IRF9 and 24 h for ubiquitin. Integrated phosphor signals are reported for IRF9 and ubiquitin; data are presented as the ratio of radioactivity in tumor: normal tissue blots (mean $\pm$ SE) for a given organ of origin with or without normalization to ubiquitin. Additional information including pathological characterization of tumors, sources of cell lines, and preparation of positive and negative controls appearing on the blot (catalogue number 7840-1, lot 9120890) can be obtained from Clontech Laboratories, Inc. Detailed data sets are available as supplemental material.[1]

RESULTS

Derivation of Paclitaxel-resistant Cell Lines. We derived paclitaxel-resistant clonal sublines of MCF-7 breast adenocarcinoma cells through a Luria-Delbrück fluctuation analysis-style selection protocol (17). Cells were subsequently cultured in the absence of drug. We obtained a mean of 7.4 colonies/1 $\times$ 10^6 cells in each of 15 populations [range, 0.4–25.6 colonies/1 $\times$ 10^6 cells; variance, 39.9 (colonies/1 $\times$ 10^6 cells)^2]. These results suggest that paclitaxel resistance arose independently in each population, as indicated by the relatively high ratio of variance:mean (5.4), and by the low rate of occurrence of surviving colonies in a control selection of progenitor cells (1 per 30 populations of 2000 cells each). The apparent rate of variation conferring resistance was 1.7 $\times$ 10^{-6} per cell generation, consistent with results from previous selections (16, 26).

Clonal sublines were derived from surviving colonies in each of the 15 populations. Cytotoxicity assays (72 h) with paclitaxel demonstrated a modest increase in IC_{50} averaging 2.2-fold (range, 0.9- to 4.8-fold) in the 53 sublines (data for representative variants are listed in Table 1). Representative dose-response curves with paclitaxel for parental MCF-7 cells and variant 11C9 are shown (Fig. 1). Modest cross-resistance to doxorubicin (2- to 5-fold) was observed in 4 (22%) of 18 variants, and cross-resistance to vinblastine was observed in 2 (33%) of 6 variants tested (Table 1). There was no correlation between resistance to paclitaxel and other agents in short-term cytotoxicity assays. Interestingly, when resistance was measured in clonogenic assays, we observed marked resistance to paclitaxel in 2 of 6 variants (11C9 and 7H8; Table 1; Fig. 1*B*). 11C9, the most resistant variant, exhibited cross-resistance to vinblastine (Fig. 1*C*), but not to doxorubicin (<2-fold) in clonogenic assays and was chosen for further analysis.

Lack of Known Mechanisms of Drug Resistance. Resistance to paclitaxel in MCF-7 variants could not be explained by altered cellular accumulation of paclitaxel (Table 1), implying a lack of altered binding sites. In principle, selection with paclitaxel can favor tubulin mutations that decrease the inherent stability of microtubules. However, microtubule instability correlates with collateral sensitivity to *Vinca* alkaloids, such as vinblastine, which bind tubulin monomers (27). Because variant 11C9 was cross-resistant to vinblastine in clonogenic assays, paclitaxel-resistance in this variant was unlikely to be the result of changes in tubulin. In addition, analysis of cell cycle response to paclitaxel (below) indicated that 11C9 cells did not have alterations in microtubular function, which would be expected to decrease the effectiveness of paclitaxel in eliciting cell cycle arrest.

The lack of cell accumulation differences for [^{3}H]paclitaxel also suggested the absence of *MDR1* Pgp. To confirm, Pgp function was determined directly using ^{99m}Tc-Sestamibi, a highly sensitive probe of Pgp transport activity (28). Although modest differences in tracer accumulation were observed among the variants, there was no enhancement of radiotracer accumulation with GF120918, a specific inhibitor of Pgp function (23). In addition, the pattern of drug resist-

Table 1 *Survey of drug-resistance characteristics for representative variants*

Cytotoxicity assays (72 h) were performed with paclitaxel, doxorubicin, and vinblastine. The IC_{50}s measured in these assays are reported for the parental line, and fold increase in IC_{50} relative to the parental line is listed for the variant lines. Accumulation of [^{3}H]paclitaxel was measured after 4 h of incubation, at which time maximal accumulation had occurred. ^{99m}Tc-Sestamibi accumulation was measured in the presence and absence of GF120918, a specific inhibitor of MDR1 Pgp.

Cell line	Fold increase in IC_{50}			CFU 100 nM paclitaxel (colonies/10^6 cells seeded)	[^{3}H]paclitaxel accumulation (pmol/mg protein)	^{99m}Tc-Sestamibi accumulation (fmol/mg protein/n_{M_o})[a]	^{99m}Tc-Sestamibi + GF120918 (fold increase)
	Paclitaxel	Doxorubicin	Vinblastine				
1C10	1.9	1.4				153 $\pm$ 21	1.2
2D3	1.8	3.7	0.9	0	169 $\pm$ 38	32 $\pm$ 5	0.9
2G11	2.3	2.5	2.5	3 $\pm$ 2	192 $\pm$ 68	90 $\pm$ 6	1.0
3H10	3.0	0.7				96 $\pm$ 2	0.8
5B9	2.8	1.5				84 $\pm$ 4	1.2
5G1	2.6	1.1				76 $\pm$ 1	0.8
6G5	3.1	1.7				83 $\pm$ 8	1.1
7H8	4.8	1.2	1.2	24 $\pm$ 7	157[b]	66 $\pm$ 11	1.0
8G4	2.9	1.4				48 $\pm$ 5	0.9
9G3	1.0	0.9				82 $\pm$ 3	0.8
11C9	3.0	2.7	1.0	103 $\pm$ 19	191 $\pm$ 32	77 $\pm$ 3	0.9
11F4	2.8	0.4				80 $\pm$ 13	1.1
12A9	1.6	1.8					
12G5	3.2	2.4	3.2	0	176 $\pm$ 15	80 $\pm$ 3	1.0
13G12	2.6	0.7				61 $\pm$ 2	1.1
14C7	3.1	1.4				107 $\pm$ 16	1.1
14D5	1.9	1.3				44 $\pm$ 2	1.0
15A2	4.4	0.2	1.1	0.3 $\pm$ 0.5	156 $\pm$ 6	52 $\pm$ 13	0.8
Parent	7.2 nM	870 nM	9.7 nM	1.4 $\pm$ 0.5	178 $\pm$ 8	90 $\pm$ 9	1.0

[a] n_{M_o}, total concentration of Tc-Sestamibi in the extracellular buffer.
[b] Single determination; others are mean of triplicates; errors represent SE.

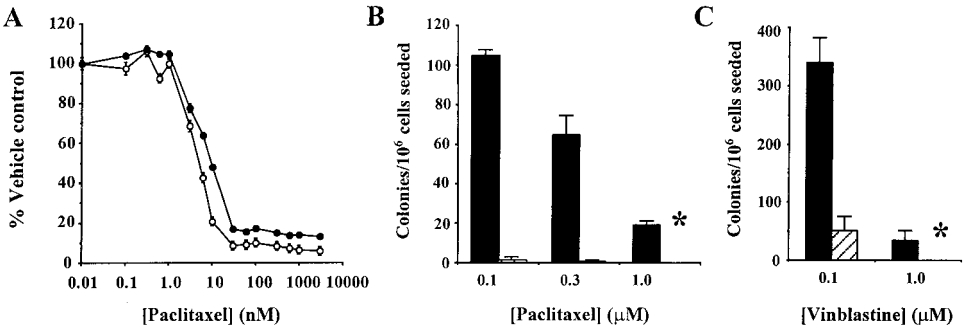

Fig. 1. *A*, paclitaxel concentration-response curve (72 h) for parental cells (○) and variant 11C9 cells (●); $n = 3$; *error bars*, SD when larger than symbol). *B* and *C*, characterization of drug resistance by colony formation assays. Number of colonies/10^6 cells seeded for parental cells (▨) and variant 11C9 cells (■) treated 7 days with (*B*) paclitaxel or (*C*) vinblastine, followed by 21 days of recovery in medium without drug. Plating efficiency was 85–90% for both lines. Values represent mean of triplicate determinations (except 0.1 μM paclitaxel, for which $n = 9$, representing 3 experiments); *error bars*, SE; ∗, average of <1 colony observed.

ance observed in clonogenic assays with 11C9 cells also ruled out involvement of *MDR1* Pgp, which would be expected to confer resistance to doxorubicin as well as to paclitaxel and vinblastine (29). Pgp and MRP1, a related protein that also mediates multidrug resistance (30), were undetectable by Western blot in parental MCF-7 cells and those variants tested (Fig. 2).

Untreated MCF-7 cells and sublines, including 11C9, were surveyed by Western blots (Fig. 2) for correlation between paclitaxel resistance and expression of proteins reported to mediate resistance to paclitaxel (reviewed in Refs. 7, 8). Paclitaxel induces phosphorylation of bcl-2 (31), and, in MCF-7 cells, bcl-2 and bcl-x_L have been correlated with resistance to paclitaxel (9, 12, 32). However, other studies suggest that apoptotic response to paclitaxel may be independent of bcl-2 levels (33) or phosphorylation state (34). Although our untreated cell lines exhibited large differences in the level of bcl-2 expression among the variants, neither bcl-2 nor bcl-x levels correlated with paclitaxel resistance. Up-regulation of cyclin-dependent kinase inhibitor p21/cip-1 via overexpression of ErbB2 has been shown to mediate resistance to paclitaxel in MDA-MB-435 breast cancer cells (35), and overexpression of p21 has been reported to favor entry into a SLP rather than cell death (13). However, we found no differences among the MCF-7 sublines in expression of p21 or a related cyclin-dependent kinase inhibitor p27/kip. Although levels of the tumor suppressor p53 differed somewhat among the MCF-7 variants tested, no correlation was evident between levels of p53 and resistance to paclitaxel, consistent with evidence that paclitaxel induces cell death through a p53-independent pathway in cells arrested in G_2-M (36). Western blots confirmed the absence of caspase-3 (37, 38) in MCF-7 cells (data not shown) and showed equal levels of caspase-7 in MCF-7 cells and sublines.

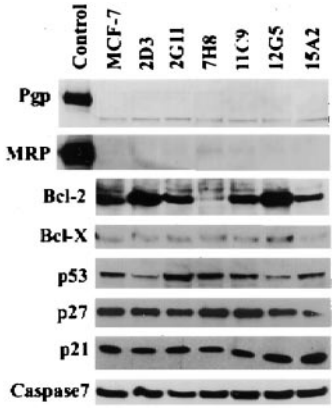

Fig. 2. Expression of candidate drug resistance mediators, cell cycle, and apoptotic regulatory proteins in untreated asynchronous cultures of MCF-7 parental cells and six paclitaxel-resistant MCF-7 variants. Western blots were prepared as in "Materials and Methods."

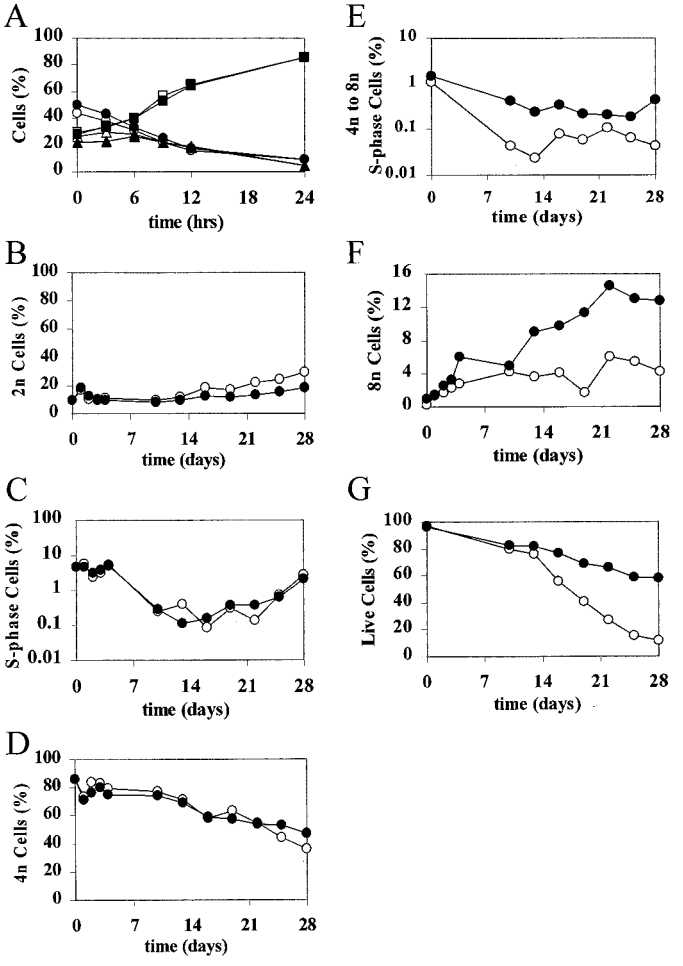

Fig. 3. *A*, pattern of cell cycle arrest throughout the first 24 h of exposure to paclitaxel (100 nM) for parental MCF-7 cells (*open symbols*) and 11C9 variant (*closed symbols*). Cells were fixed, stained with PI, and analyzed by flow cytometry as described in "Materials and Methods. A representative experiment is shown. *2n* (*circles*); *S-phase* (*triangles*); *4n* (*squares*). *B–G*, flow cytometric analysis of parental MCF-7 cells (*open symbols*) and 11C9 variant (*closed symbols*) during *recovery* from paclitaxel exposure (7 days, 100 nM). Day 0, day of removal of paclitaxel and replacement with medium without drug. Cells were pretreated for 4 h with BrdUrd prior to being fixed and stained with PI and FITC-anti-BrdUrd. Data in *A* and *G* expressed as percentage of total events recorded; data in *B–F* expressed as percentage of live cells. *B*, cells with DNA content of 2n. *C*, cells in S phase as determined by BrdUrd incorporation, progressing from 2n to 4n. *D*, cells with 4n DNA content. *E*, cells in S phase as determined by BrdUrd incorporation, progressing from 4n to 8n. *F*, cells with 8n DNA content. *G* , cells with DNA content ≥ 2n (live cells).

Cell Cycle Response to Paclitaxel. To determine whether resistance to paclitaxel in clonogenic assays might arise from a difference in cell cycle response to paclitaxel, we measured the cell cycle distribution of adherent MCF-7 and 11C9 cells at intervals throughout a clonogenic assay (Fig. 3). Untreated MCF-7 and 11C9 cells (time 0)

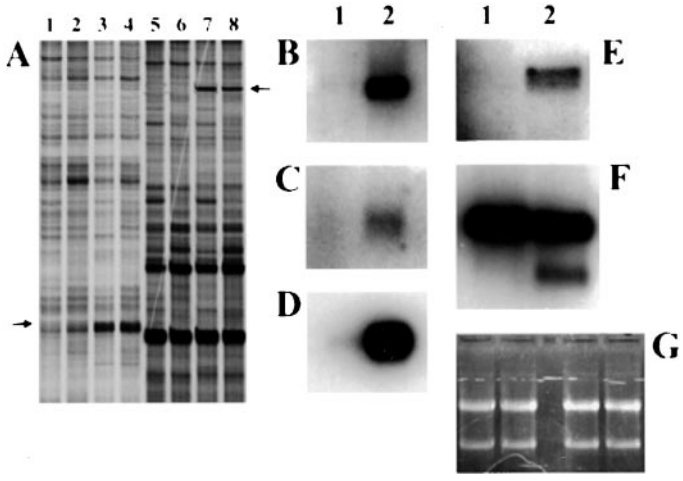

Fig. 4. *A*, representative autoradiograph of differential display showing separation of random primed products on 6% polyacrylamide gels. Shown are MCF-7 cells (*Lanes 1, 2, 5,* and *6*) and 11C9 cells (*Lanes 3, 4, 7,* and *8*) both untreated (*Lanes 1, 3, 5,* and *7*) and 15 days after removal of paclitaxel (*Lanes 2, 4, 6,* and *8*). *Arrows*, confirmed differences: *lower left*, MxA protein; *upper right*, KIAA0069. *B–F*, Northern blots of cloned differences (*left lane*, MCF-7 cells; *right lane*, 11C9 cells). *B*, MxA; *C*, hepatitis C-associated microtubular aggregate protein; *D*, IFI27; *E*, unknown 7-kb transcript; *F*, KIAA0069. *G*, representative formaldehyde gel demonstrating equal loading of RNA.

had similar cell cycle profiles (Fig. 3*A*). On addition of paclitaxel [100 nM (Fig. 3*A*) or 10 nM (data not shown)], cell cycle arrest in MCF-7 and 11C9 was essentially identical over the first 24 h. Prolonged exposure to paclitaxel (100 nM × 7 days) and subsequent culture in drug-free medium (Fig. 3; days 0–28) also demonstrated little difference between MCF-7 and 11C9 cells in the 2*n*, S phase, and the 4*n* populations at all points (Fig. 3, *B–D*). 11C9 cells were more likely to endoreduplicate and enter a polyploid state (Fig. 3, *E* and *F*), suggesting a potential defect in the checkpoint regulating G_1 to S phase transition. In both cell lines, emergence of a diploid S-phase population and a slight increase in the fraction of 2*n* cells was noted concurrent with microscopic observation of colony formation (days 25 and 28). On the basis of biochemical and morphological markers, cell death in response to paclitaxel was necrotic rather than apoptotic in both MCF-7 and 11C9 cells (data not shown), taking place gradually over the several weeks in drug-free medium. 11C9 cells were resistant to cell death throughout the recovery phase, having a greater fraction of adherent cells with intact DNA (≥2*n*; Fig. 3*G*) as well as more adherent cells that excluded trypan blue (2- to 3-fold more on day 21; data not shown). Although the fraction of live diploid cells entering S-phase is the same for MCF-7 and 11C9 cells throughout the experiment, the absolute number of live 11C9 cells is considerably greater at the onset of colony formation, resulting in a greater number of proliferating diploid 11C9 cells. Overall, these results suggest resistance to cell death, not increased ability to resume proliferation, as the main cause of increased clonogenicity of 11C9 cells after exposure to paclitaxel.

Differential Display. To identify differences in gene expression associated with resistance to paclitaxel in 11C9 cells, we compared mRNA expression patterns in MCF-7 and 11C9 cells by differential display (Ref. 39; Fig. 4*A*). RNA was prepared from (*a*) untreated asynchronous cultures of each and (*b*) paclitaxel-treated cultures of each 15 days after removal of paclitaxel (day 23 of protocol). The latter samples were taken at a time when cell proliferation was first observed by light microscopy and cells were primarily in a 4*n* state with ~10% of 11C9 cells progressing through abnormal S phase to 8*n* (as observed in Fig. 3 and related experiments). Only 21 reproducible differences were noted between 11C9 and parental MCF-7 cells using 240 primer combinations (designed to theoretically sample ~24,000 transcripts), which suggested very limited genetic variation between these cell lines. Of the five differences in gene expression between 11C9 and MCF-7 cells confirmed by Northern blots (Fig. 4, *B–G*), four represented overexpression of a transcript in 11C9 cells, and one was the result of a COOH-terminal truncation of a transcript (predicted transmembrane protein KIAA0069) through mutation to produce a stop codon. All of the differences confirmed by Northern blots were equally evident in asynchronous and paclitaxel-treated cultures (Fig. 4*A* and data not shown). Of the four overexpressed transcripts, three matched entries in GenBank: MxA protein (MxA), hepatitis C-associated microtubular aggregate protein (p44), and IFNα-inducible p27 (IFI27). Among these proteins only MxA has a known function, which is to confer cellular resistance to viral infection. All three, however, have been shown to be inducible by type I IFNs (40–42).

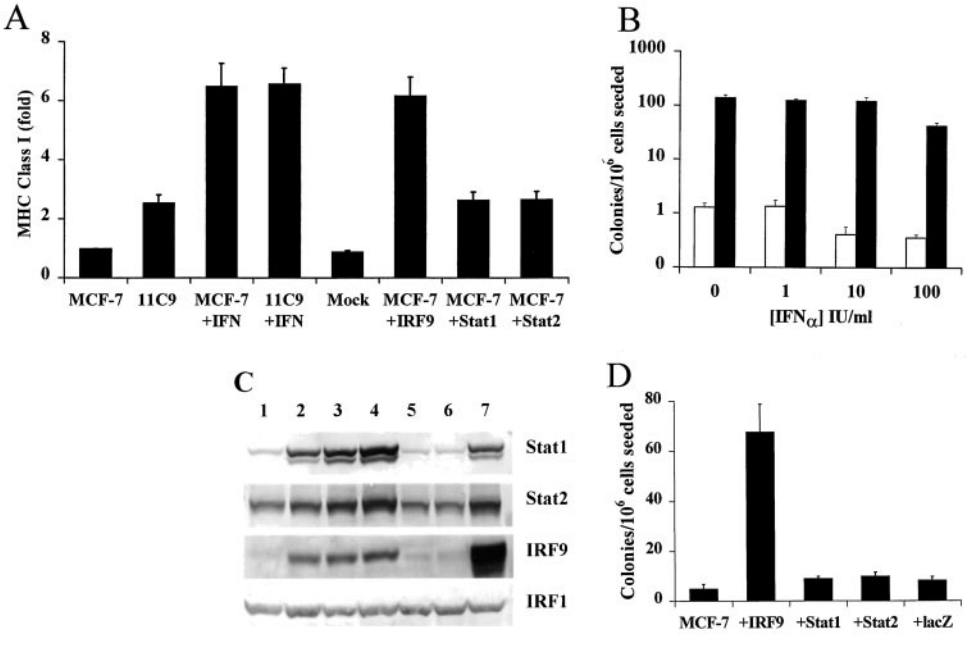

Fig. 5. *A*, MHC class I expression as determined by flow cytometry in untreated and treated MCF-7 cells [treated 72 h with 1000 units/ml IFNα or transfected with IRF9, Stat1, Stat2 or transfection reagent alone (mock)] and untreated and treated 11C9 cells (treated 72 h with 1000 units/ml IFNα). Data are presented as the ratio of mean fluorescence intensity of treated cells:untreated parental cells in the same experiment. *Bars*, mean ± SE for representative experiments. *B*, effect of IFNα on colony forming efficiency of MCF-7 and 11C9 cells. Number of colonies/10^6 cells seeded for parental cells (□) and variant 11C9 cells (■). *Values*, mean of triplicate determinations ± SE. *C*, Western blots for expression of Stat1, Stat2, IRF9, and IRF1. *Lane 1*, untreated MCF-7 cells; *Lane 2*, untreated 11C9 cells; *Lane 3*, MCF-7 cells treated 72 h with 1000 IU/ml IFNα; *Lane 4*, 11C9 cells treated 72 h with 1000 IU/ml IFNα; *Lane 5*, untransfected MCF-7 cells; *Lane 6*, mock transfected MCF-7 cells (transfection reagent only); *Lane 7*, MCF-7 cells 72 h after transfection with IRF9. *D*, effect of transient transfection with IRF9, Stat1, Stat2, or β-galactosidase (*lacZ*) on colony-forming efficiency in MCF-7 cells treated with 100 nM paclitaxel.

Examination of Type I IFN Pathway. MHC Class I protein, known to be induced by both types I and II IFNs (43, 44), was determined by flow cytometry (Fig. 5*A*) to be overexpressed in 11C9 cells (2.5-fold) relative to MCF-7 cells. IFNα increased expression of class I in both cell lines to a level 2.5-fold greater than that in untreated 11C9 cells. However, receptor-mediated activation of type I IFN signaling was ruled out as the source of paclitaxel resistance in 11C9 cells based on the absence of IFN in 11C9 culture supernatants (as determined by CPE assay; data not show) and the inability of IFNα to confer paclitaxel resistance on MCF-7 cells (Fig. 5*B*). Type I IFN signaling was intact in MCF-7 and 11C9 cells, as evidenced by the ability of IFNα to protect MCF-7 and 11C9 cells from virus-mediated cell death in CPE assays (data not shown).

Signaling to the nucleus by type I IFNs is mediated by ISGF3, a heterotrimer consisting of phospho-Stat1, phospho-Stat2, and an IFN regulatory factor IRF9/p48/ISGF3γ (IRF9; Ref. 45). Stat1 and Stat2 are phosphorylated by Janus kinases Jak1 and Tyk2 upon association of IFN with the type I IFN receptor (IFNAR). IRF9 contains an N-terminal bipartite nuclear retention signal (46), and is the primary DNA binding protein of ISGF3, recognizing the IFN-responsive promoter element (ISRE) in type I IFN regulated genes (47). Western blot analysis demonstrated that, relative to parental MCF-7 cells, 11C9 cells overexpressed IRF9 and Stat1 (both 6–10 fold) as well as Stat2 (2-fold; Fig. 5C). MCF-7 cells treated with IFNα exhibited a pattern of expression similar to untreated 11C9 cells, whereas 11C9 cells treated with IFNα showed a slightly amplified pattern. In contrast to IRF9, IRF1, a related IFN regulatory factor (48), was not overexpressed under any of these conditions.

Transfection with IRF9 Reproduces Gene Expression Pattern and Drug Resistance. Because IRF9 is the primary DNA binding component of ISGF3 (47), overexpression of IRF9 might induce expression of a subset of IFN-inducible genes, thereby conferring the drug-resistant phenotype. To test this hypothesis, MCF-7 cells were transfected with wild-type IRF9. Transient transfection with IRF9 was found to induce expression of Stat1, Stat2 (Fig. 5C, *Lane 7*), and MHC class I (Fig. 5*A*), but not IRF1 (Fig. 5*C*) or IFN (determined by CPE assay; data not shown). Transient transfection of MCF-7 cells with IRF9 also produced 13-fold resistance to paclitaxel (100 nM; Fig. 5*D*) and 3.3-fold resistance to vinblastine (1.0 μM), but no resistance to doxorubicin, recapitulating the resistance phenotype of 11C9 cells. Transient transfection of MCF-7 cells with Stat1 p91 or Stat2, did not confer resistance to paclitaxel (Fig. 5*D*), although these transfections with Stat1 or Stat2 produced 2.6-fold increases in MHC class I expression (Fig. 5*A*). These transfection data provide evidence that the multidrug-resistance phenotype observed in variant 11C9 is linked to IRF9 overexpression.

Overexpression of IRF9 in Breast and Uterine Tumors. To begin to characterize IRF9 expression in clinical specimens, we compared IRF9 expression levels in donor-matched pairs of untreated human tumors and normal organ tissues (Fig. 6)[4] using a commercial tissue blot. As a group, breast tumors overexpressed IRF9 3-fold relative to donor-matched normal breast tissue, and a subset of tumors highly overexpressed IRF9 [IRF9 expression: tumor:normal tissue ratio, 2.83 $\pm$ 0.53 (mean $\pm$ SE); range, 1.27 to 5.64; ratio $>$ 2.0 in six of nine tumors; IRF9 expression normalized to ubiquitin: tumor: normal tissue ratio, 2.83 $\pm$ 0.96 (mean $\pm$ SE); range, 0.97–10.48; ratio $>$ 2.0 in three of nine tumors]. Uterine tumors overall also exhibited significant IRF9 overexpression with a subset highly overexpressing the factor [IRF9 expression: tumor:normal tissue ratio, 2.61 $\pm$ 0.99 (mean $\pm$ SE); range, 1.04–5.81; ratio $>$ 2.0 in three of seven tumors; IRF9 expression normalized to ubiquitin: tumor/normal tissue ratio, 2.88 $\pm$ 1.09 (mean $\pm$ SE); range, 0.7–5.03; ratio $>$ 2.0 in five of seven tumors]. Although breast tumors in this data set were primarily derived from epithelial cell types (six infiltrating ductal carcinomas, one lobular carcinoma, one mucinous adenocarcinoma, and one medullary carcinoma), and the uterine "tumors" represented various abnormal cell types (three benign tumors, two squamous cell carcinomas, and two adenocarcinomas), IRF9 overexpression did not segregate into any specific cell types in the data set. Breast and uterine tumors were the only tested tumor types to show systematic overexpression of IRF9.

DISCUSSION

Enforced overexpression of the IFN regulatory factor IRF9 in drug-sensitive MCF-7 breast cancer cells conferred paclitaxel- and vinblastine-resistance and recapitulated the pattern of IFN-inducible genes observed in drug-resistant cells. In contrast, treatment of drug-sensitive cells with IFNα did not confer drug resistance, despite induction of a pattern of gene expression similar to that produced by overexpression of IRF9. These results demonstrate a new role for IRF9 in conferring resistance to microtubule-directed antitumor agents.

IRF9 Overexpression Confers Resistance to Antimicrotubule Agents. 11C9 cells demonstrated overexpression of proteins associated with type I IFN signaling, including all three subunits of the ISGF3 transcriptional activator (IRF9, Stat1, and Stat2) as well as IFN-inducible MxA, IFI27, p44, and MHC class I proteins. Because IRF9 is the major DNA-binding protein in the ISGF3 complex (47), we predicted that IRF9 overexpression might activate IFN-responsive genes through increased occupancy of binding sites in promoter elements. Enforced overexpression of IRF9 in parental MCF-7 cells indeed produced a pattern of gene expression mimicking that observed in 11C9 cells and IFNα-treated MCF-7 cells. However, in MCF-7 cells, transfection only with IRF9, but not Stat1 or Stat2, reproduced the drug-resistance phenotype observed in 11C9 cells. Our results suggested that IRF9 within untreated 11C9 cells and IRF9-transfected MCF-7 cells did not produce its effect through the ISGF3 heterotrimer typical of type I IFN signaling. Most notably, treatment of MCF-7 cells with IFNα at low concentrations produced no effect on resistance to paclitaxel and, at high concentrations, produced the expected cytostatic effect (45), rather than inducing paclitaxel resistance.

It is unclear whether IRF9 acts alone or as a complex with other proteins such as Stats to activate transcription of IFN-inducible genes in MCF-7 cells. IRF9 can access the nucleus in the absence of IFN by virtue of an NH_2-terminal bipartite nuclear retention signal (46). Stats 1 and 2 are cytosolic, and nuclear localization of IRF9 is reduced in cells overexpressing Stat2 (46). Previous studies have shown that overexpression of IRF9 by transfection results in the induction of several IFN-inducible genes (49), which suggests that IRF9-induced transcription may be mediated by IRF9 alone. However, the binding of IRF9 alone to IFN-responsive promoter elements has been shown to be weak relative to the binding of ISGF3 (50). Experiments are in progress to determine the mechanism of activation of IFN-inducible genes by IRF9 in MCF-7 cells.

Our data indicate that IFN signaling has been activated in 11C9 cells in the absence of IFN. Several other mechanisms of induction of IFN-responsive genes have been described. Retinoids and interleukin-6 have been reported to induce overexpression of IRF9 (51, 52). In addition, decreased expression of IRF2, a repressor of transcription of many IFN-responsive genes, has been shown to result in increased expression of IFN-responsive genes in $IRF2^{-/-}$ mice (53). Overexpression of IFN-inducible genes also has been reported in confluent and senescent cultured human mammary epithelial (HME) cells (but

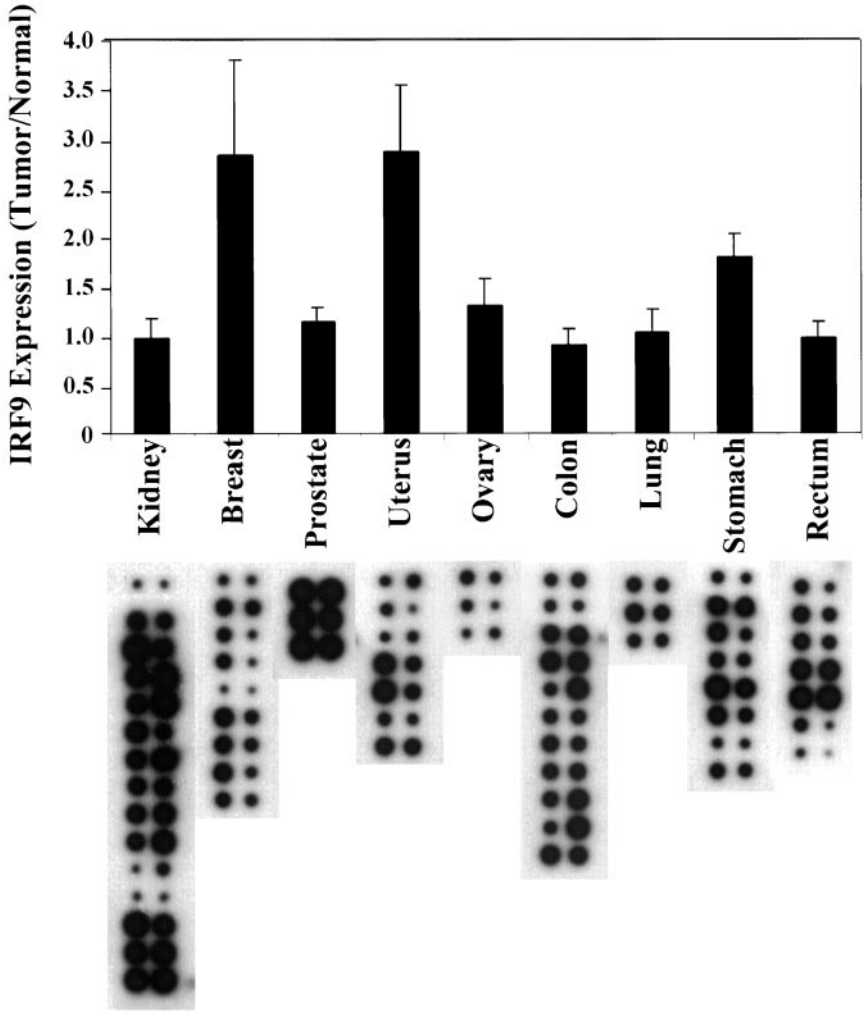

Fig. 6. Summary of IRF9 mRNA expression in matched tumor/normal tissue blots from various organs. *Columns*, IRF9 expression as the ratio of tumor:normal tissue blots (mean ± SE) for a given organ of origin normalized to ubiquitin in each sample. *Below each organ*, autoradiographs of blots of IRF9 expression for pairs of tumor (*left*) and matched normal organ tissue (*right*). Supplemental material with complete autoradiographs and quantitation of IRF9 and ubiquitin, as well as clinical data for each tumor, is available.[1]

not normally-proliferating HME cells), again suggesting that signals other than IFN may induce expression of IFN-responsive genes (54).

Surprisingly, many of the characteristics of the resistance phenotype conferred by IRF9 in MCF-7 cells appear essentially opposite to the typical effects of IFNs. IFNs have primarily been associated with antiproliferative function and initiation of apoptosis (45). Although many IFN-inducible proteins, including MxA, inhibit cell death from viral infection (55), their primary action appears to be inhibition of virus replication, rather than prevention of apoptosis or necrosis. Hepatitis C-associated microtubular aggregate protein p44 has potential to contribute to protection from antimicrotubule agents by virtue of its association with microtubules (41). However, the function of p44 is unknown, as is the function of IFI27. Understanding the mechanism of resistance to paclitaxel conferred by IRF9 will require a detailed examination of the effect of IRF9 overexpression on proteins mediating arrest and cell death in response to paclitaxel, as well as the identification of other IFN-inducible genes up-regulated by IRF9.

IFN-responsive Genes, Drug Resistance, and Breast Cancer. Using a donor-matched array of cDNA prepared from untreated human tumor and normal organ tissue from a variety of organs, we observed overexpression of IRF9 in a subset of breast and uterine tumors. These data strengthen an emerging pattern of overexpression of IFN-responsive genes in breast cancer. IRF9, Stat1, hepatitis C-associated microtubular aggregate protein p44, IFI27, and MHC class I, among others, have been reported to be overexpressed in approximately one-half of untreated breast tumors examined using cDNA microarrays (54, 56). Although cDNA prepared from whole tissue can be criticized for reflecting a variety of cell types, several studies have directly identified overexpression of IFN-responsive genes such as Stat1 and IFI27 in breast tumor cells when examined by immunohistochemistry (42, 54, 57, 58). It is possible that IRF9 overexpression in tumors *in vivo* may be associated with resistance to antimicrotubule agents; however, no outcome data were available for the samples included in the commercial blot. Direct correlation of tumor IRF9 levels with outcome in patients treated with antimicrotubule agents remains to be done to prove whether IRF9 overexpression is associated with treatment failure or recurrence of disease clinically.

Overall, we conclude that overexpression of IRF9 is involved in regulating downstream IFN-responsive genes in human breast tumor cells independent of IFN. Our data suggest that IRF9 may be associated with drug resistance and has the potential to be a surrogate marker of response.

REFERENCES

1. Hoyt, M. A. Exit from mitosis: spindle pole power. Cell, *102:* 267–270, 2000.
2. Sorger, P. K., Dobles, M., Tournebize, R., and Hyman, A. A. Coupling cell division and cell death to microtubule dynamics. Curr. Opin. Cell Biol., *9:* 807–814, 1997.
3. Waters, J. C., Chen, R-H., Murray, A. W., and Salmon, E. D. Localization of Mad2 to kinetochores depends on microtubule attachment, not tension. J. Cell. Biol., *141:* 1181–1191, 1998.
4. Chang, B-D., Vroude, E. V., Dokmanovic, M., Zhu, H., Ruth, A., Xuan, Y., Kandel, E. S., Lausch, E., Christov, K., and Roninson, I. B. A senescence-like phenotype distinguishes tumor cells that undergo terminal proliferation arrest after exposure to anticancer agents. Cancer Res., *59:* 3761–3767, 1999.

5. Pines, J. Cell cycle. Checkpoint on the nuclear frontier. Nature (Lond.), *397:* 104–105, 1999.
6. Wang, L. G., Liu, X. M., Kreis, W., and Budman, D. R. The effect of antimicrotubule agents on signal transduction pathways of apoptosis: a review. Cancer Chemother. Pharmacol., *44:* 355–361, 1999.
7. Wang, T-H., Wang, H-S., and Soong, Y-K. Paclitaxel-induced cell death. Cancer (Phila.), *88:* 2619–2628, 2000.
8. Dumontet, C., and Sikic, B. Mechanisms of action of and resistance to antitubulin agents: microtubule dynamics, drug transport, and cell death. J. Clin. Oncol., *17:* 1061–1070, 1999.
9. Huang, Y., Ray, S., Reed, J. C., Ibrado, A. M., Tang, C., Nawabi, A., and Bhalla, K. Estrogen increases intracellular p26Bcl-2 to p21Bax ratios and inhibits Taxol-induced apoptosis of human breast cancer MCF-7 cells. Breast Cancer Res. Treat., *42:* 73–81, 1997.
10. Li, W., Fan, J., Banerjee, D., and Bertino, J. R. Overexpression of p21(waf1) decreases G_2-M arrest and apoptosis induced by paclitaxel in human sarcoma cells lacking both p53 and functional Rb protein. Mol. Pharmacol., *55:* 1088–1093, 1999.
11. Wahl, A., Donaldson, K., Fairchild, C., Lee, F., Foster, S., Demers, G., and Galloway, D. Loss of normal p53 function confers sensitization to Taxol by increasing G_2/M arrest and apoptosis. Nat. Med., *2:* 72–79, 1996.
12. Sumantran, V. N., Ealovega, M. W., Nunez, G., Clarke, M. F., and Wicha, M. S. Overexpression of Bcl-XS sensitizes MCF-7 cells to chemotherapy-induced apoptosis. Cancer Res., *55:* 2507–2510, 1995.
13. Chang, B-D., Xuan, Y., Broude, E. V., Zhu, H., Shott, B., Fang, J., and Roninson, I. B. Role of p53 and $p21^{waf1/cip1}$ in senescence-like terminal proliferation arrest induced in human tumor cells by chemotherapeutic drugs. Oncogene, *18:* 4808–4818, 1999.
14. Bunz, F., Dutriaux, A., Lengauer, C., Waldman, T., Zhou, S., Brown, J., Sedivy, J., Kinzler, K., and Vogelstein, B. Requirement for p53 and p21 to sustain G_2 arrest after DNA damage. Science (Wash. DC), *282:* 1497–1501, 1998.
15. Akiyama, S. I., Fojo, A., Hanover, J. A., Pastan, I., and Gottesman, M. M. Isolation and genetic characterization of human KB cell lines resistant to multiple drugs. Somatic Cell Mol. Genet., *11:* 117–126, 1985.
16. Dumontet, C., Duran, G., Steger, K., Beketic-Oreskovic, L., and Sikic, B. Resistance mechanisms in human sarcoma mutants derived by single-step exposure to paclitaxel (Taxol). Cancer Res., *56:* 1091–1097, 1996.
17. Luria, S., and Delbrück, M. Mutations of bacteria from virus sensitivity to virus resistance. Genetics, *28:* 491–511, 1943.
18. Kendal, W. S., and Frost, P. Pitfalls and practice of Luria-Delbrück fluctuation analysis: a review. Cancer Res., *48:* 1060–1065, 1988.
19. Sharma, V., Crankshaw, C., and Piwnica-Worms, D. Effects of multidrug resistance (*MDR1*) Pgp expression levels and coordination metal on the cytotoxic potency of multidentate (N_4O_2) ethylenediamine-bis[propyl(R-benzylimino)]metal(III) cations. J. Med. Chem., *39:* 3483–3490, 1996.
20. Luker, G., Rao, V., Crankshaw, C., Dahlheimer, J., and Piwnica-Worms, D. Characterization of phosphine complexes of technetium (III) as transport substrates of the multidrug resistance (MDR1) P-glycoprotein and functional markers of P-glycoprotein at the blood-brain barrier. Biochemistry, *36:* 14218–14227, 1997.
21. Rao, V., Dahlheimer, J., Bardgett, M., Snyder, A., Finch, R., Sartorelli, A., and Piwnica-Worms, D. Choroid plexus epithelial expression of MDR1 P-glycoprotein and multidrug resistance-associated protein contribute to the blood-cerebrospinal fluid drug-permeability barrier. Proc. Natl. Acad. Sci. USA, *96:* 3900–3905, 1999.
22. Piwnica-Worms, D., Rao, V., Kronauge, J., and Croop, J. Characterization of multidrug-resistance P-glycoprotein transport function with an organotechnetium cation. Biochemistry, *34:* 12210–12220, 1995.
23. Hyafil, F., Vergely, C., Du Vignaud, P., and Grand-Perret, T. *In vitro* and *in vivo* reversal of multidrug resistance by GF120918, an acridonecarboxamide derivative. Cancer Res., *53:* 4595–4602, 1993.
24. Horvath, C. M., and Darnell, J., J. E. The antiviral state induced by α interferon and γ interferon requires transcriptionally active Stat1 protein. J. Virol., *70:* 647–650, 1996.
25. Altshul, S. F., Gish, W., Miller, W., Meyers, E., and Lipman, D. J. Basic local alignment search tool. J. Mol. Biol., *215:* 403–410, 1990.
26. Chen, G., Duran, G., Mangili, A., Beketic-Oreskovic, L., and Sikic, B. MDR 1 activation is the predominant resistance mechanism selected by vinblastine in MES-SA cells. Br. J. Cancer, *83:* 892–898, 2000.
27. Giannakakou, P., Sackett, D., Kang, Y-K., Zhan, Z., Buters, J., Fojo, T., and Poruchynsky, M. Paclitaxel-resistant human ovarian cancer cells have mutant β-tubulins that exhibit impaired paclitaxel-driven polymerization. J. Biol. Chem., *272:* 17118–17125, 1997.
28. Sharma, V., and Piwnica-Worms, D. Metal complexes for therapy and diagnosis of drug resistance. Chem. Rev., *99:* 2545–2560, 1999.
29. Ambudkar, S., Dey, S., Hrycyna, C., Ramachandra, M., Pastan, I., and Gottesman, M. Biochemical, cellular, and pharmacological aspects of the multidrug transporter. Annu. Rev. Pharmacol. Toxicol., *31:* 361–398, 1999.
30. Cole, S. P. C., Bhardwaj, G., Gerlach, J. H., Mackie, J. E., Grant, C. E., Almquist, K. C., Stewart, A. J., Kurz, E. U., Duncan, A. M. V., and Deeley, R. G. Overexpression of a transporter gene in a multidrug-resistant human lung cancer cell line. Science (Wash. DC), *258:* 1650–1654, 1992.
31. Scatena, C., Stewart, Z., Mays, D., Tang, L., Keefer, C., Leach, S., and Pietenpol, J. Mitotic phosphorylation of bcl-2 during normal cell cycle progression and Taxol-induced growth arrest. J. Biol. Chem., *273:* 30777–30784, 1998.
32. Srivastava, R. K., Srivastava, A. R., Korsmeyer, S. J., Nesterova, M., Cho-Chung, Y. S., and Longo, D. L. Involvement of microtubules in the regulation of Bcl2 phosphorylation and apoptosis through cyclic AMP-dependent protein kinase. Mol. Cell. Biol., *18:* 3509–3517, 1998.
33. Gan, Y., Wientjes, M., and Au, J. Relationship between paclitaxel activity and pathobiology of human solid tumors. Clin. Cancer Res., *4:* 2949–2955, 1998.
34. Wang, T-H., Popp, D., Wang, H-S., Saitoh, M., Mural, J., Henley, D., Ichijo, H., and Wimalasena, J. Microtubule disfunction induced by paclitaxel initiates apoptosis through both c-Jun N-terminal kinase (JNK)-dependent and -independent pathways in ovarian cancer cells. J. Biol. Chem., *274:* 8208–8216, 1999.
35. Yu, D., Jing, T., Liu, B., Yao, J., Tan, M., McDonnell, T., and Hung, M. Overexpression of ErbB2 blocks Taxol-induced apoptosis by upregulation of p21Cip1, which inhibits p34Cdc2 kinase. Mol. Cell, *2:* 581–591, 1998.
36. Woods, C. M., Zhu, J., McQueney, P. A., Bollag, D., and Lazarides, E. Taxol-induced mitotic block triggers rapid onset of a p53-independent apoptotic pathway. Mol. Med., *1:* 506–526, 1995.
37. Yang, X., Stennicke, H. R., Wang, B., Green, D. R., Janicke, R. U., Srinivasan, A., Seth, P., Salvensen, G. S., and Froelich, C. J. Granzyme B mimics apical caspases. Description of a unified pathway for *trans*-activation of executioner caspase-3 and -7. J. Biol. Chem., *273:* 34278–34283, 1998.
38. Kurokawa, H., Nishio, K., Fukumoto, H., Tomonari, A., Suzuki, T., and Saijo, N. Alteration of caspase-3 (CPP32/Yama/apopain) in wild-type MCF-7, breast cancer cells. Oncol. Rep., *6:* 33–37, 1999.
39. Liang, P., and Pardee, A. Method of differential display. Methods Mol. Genet., *5:* 3–16, 1994.
40. Ronni, T., Matikainen, S., Lehtonen, A., Palvimo, J., Dellis, J., van Eylen, F., Goetschy, J-F., Horisberger, M., Content, J., and Julkunen, I. The proximal interferon-stimulated response elements are essential for interferon responsiveness: A promoter analysis of the antiviral MxA gene. J. Interferon Cytokine Res., *18:* 773–781, 1998.
41. Kitamura, A., Takahashi, K., Okajima, A., and Kitamura, N. Induction of the human gene for p44, a hepatitis-C-associated microtubular aggregate protein, by interferon-α/β. Eur. J. Biochem., *224:* 877–883, 1994.
42. Rasmussen, U. B., Wolf, C., Mattei, M. G., Chenard, M. P., Bellocq, J. P., Chambon, P., Rio, M. C., and Basset, P. Identification of a new interferon-α-inducible gene (*p27*) on human chromosome 14q32 and its expression in breast carcinoma. Cancer Res., *53:* 4096–4101, 1993.
43. Gobin, S. J., van Zutphen, M., Woltman, A. M., and van den Elsen, P. J. Transactivation of classical and nonclassical HLA class I genes through the IFN-stimulated response element. J. Immunol, *163:* 1428–1434, 1999.
44. Friedman, R. L., and Stark, G. R. α-Interferon-induced transcription of HLA and metallothionein genes containing homologous upstream sequences. Nature (Lond.), *314:* 637–639, 1985.
45. Stark, G., Kerr, I., Williams, B., Silverman, R., and Schreiber, R. How cells respond to interferons. Annu. Rev. Biochem., *67:* 227–264, 1998.
46. Lau, J., Parisien, J-P., and Horvath, C. Interferon regulatory factor subcellular localization is determined by a bipartite nuclear localization signal in the DNA-binding domain and interaction with cytoplasmic retention factors. Proc. Natl. Acad. Sci. USA, *97:* 7278–7283, 2000.
47. Veals, S., Santa Maria, T., and Levy, D. Two domains of ISGF3-γ that mediate protein-DNA and protein-protein interactions during transcription factor assembly contribute to DNA-binding specificity. Mol. Cell. Biol., *13:* 196–206, 1993.
48. Mamane, Y., Helbroeck, C., Génin, P., Algarté, M., Servant, M. J., LePage, C., DeLuca, C., Kwon, H., Lin, R., and Hiscott, J. Interferon regulatory factors: the next generation. Gene, *237:* 1–14, 1999.
49. Bluyssen, H., Muzaffar, R., Vlieststra, R., van der Made, A., Leung, S., Stark, G., Kerr, I., Trapman, J., and Levy, D. Combinatorial association and abundance of components of interferon-stimulated gene factor 3 dictate the selectivity of interferon responses. Proc. Natl. Acad. Sci. USA, *92:* 5645–5649, 1995.
50. Bluyssen, H. A., and Levy, D. E. Stat2 is a transcriptional activator that requires sequence-specific contacts provided by stat1 and p48 for stable interaction with DNA. J. Biol. Chem, *272:* 4600–4605, 1997.
51. Matikainen, S., Ronni, T., Lehtonen, A., Sareneva, T., Melen, K., Nordling, S., Levy, D. E., and Julkunen, I. Retinoic acid induces signal transducer and activator of transcription (STAT) 1, STAT2, and p48 expression in myeloid leukemia cells and enhances their responsiveness to interferons. Cell Growth Differ., *8:* 687–698, 1997.
52. Weihua, X., Hu, J., Roy, S., Mannino, S., and Kalvakolanu, D. Interleukin-6 modulates interferon-regulated gene expression by inducing the ISGF3-γ gene using CCAAT/enhancer binding protein-β (C/EBP-β). Biochim. Biophys. Acta, *1492:* 163–171, 2000.
53. Hida, S., Ogasawara, K., Sato, K., Abe, M., Takayanagi, H., Yokochi, T., Sato, T., Hirose, S., Shirai, T., Taki, S., and Taniguchi, T. CD8(+) T cell-mediated skin disease in mice lacking IRF-2, the transcriptional attenuator of interferon-α/β signaling. Immunity, *13:* 643–655, 2000.
54. Perou, C. M., Jeffrey, S. S., van de Rijn, M., Rees, C. A., Eisen, M. B., Ross, D. T., Pergamenschikov, A., Williams, C. F., Zhu, S. X., Lee, J. C. F., Lashkar, D., Shalon, D., Brown, P. O., and Botstein, D. Distinctive gene expression patterns in human mammary epithelial cells and breast cancers. Proc. Natl. Acad. Sci. USA, *96:* 9212–9217, 1999.
55. Biron, C., and Sen, G. C. Interferons, chemokines and other cytokines. *In:* D. Knipe, P. Howley, D. Griffin, R. Lamb, M. Martin, and S. Straus (eds.), Fields Virology. Philadelphia: Lippincott, Williams, and Wilkins, 2000.
56. Perou, C. M., Sorlie, T., Eisen, M. B., van de Rijn, M., Jeffrey, S. S., Rees, C. A., Pollack, J. R., Ross, D. T., Johnsen, H., Akslen, L. A., Fluge, O., Pergamenschikov, A., Williams, C., Zhu, S. X., Lonning, P. E., Borresen-Dale, A. L., Brown, P. O., and Botstein, D. Molecular portraits of human breast tumours. Nature (Lond.), *406:* 747–752, 2000.
57. Watson, C. J., and Miller, W. R. Elevated levels of members of the STAT family of transcription factors in breast carcinoma nuclear extracts. Br. J. Cancer, *71:* 840–844, 1995.
58. Garcia, R., and Jove, R. Activation of STAT transcription factors in oncogenic tyrosine kinase signaling. J. Biomed. Sci., *5:* 79–85, 1998.